# International Journal of Analysis and Applications



## Role of Thermal Radiations in MHD Micropolar Nanofluid Flow over a Stretching/Shrinking Surface: Triple Solutions with Stability Analysis

## Khuram Rafique<sup>1</sup>, Gamal Elkahlout<sup>2,\*</sup>, Shamaila Kanwal<sup>3</sup>

<sup>1</sup>Centre of Excellence for Social Innovation and Sustainability, Institute of Engineering Mathematics,
University Malaysia Perlis, Arau, Perlis, Malaysia

<sup>2</sup>Faculty of Business Studies, Arab Open University, Riyadh, Saudi Arabia

<sup>3</sup>Department of Mathematics, University of Sialkot, Sialkot 51040, Pakistan

\*Corresponding author: g.elkahlout@arabou.edu.sa

ABSTRACT: Enhancing thermal efficiency is one of the best strategies for optimizing energy resources. As a result, researchers have been working hard to develop novel ways to maximize the results of energy use. Researchers are becoming more and more interested in nanofluids because of their distinctive thermophysical characteristics and potential uses in thermal engineering systems, heating and cooling processes, nanotechnology, and biomedicine. This study presents a numerical investigation of heat and mass transfer analysis of micropolar nanofluid flow over a stretching/shrinking surface, by incorporating an inclined magnetic field, chemical reaction, and Soret effects. A suitable methodology is adopted to transform the governing boundary layer equations of fluid flow into dimensionless nonlinear ODEs. The stability analysis method is used to resolve coupled nonlinear differential equations with MATLAB software using the Bvp4c solver. Graphs are utilized to illustrate how dimensionless physical factors affect the velocity, temperature, and concentration patterns. It was concluded that increasing the values of the radiation parameter caused a decline in the temperature profile, whereas an increment in the Soret factor enhanced the temperature profile.

#### 1. Introduction

The study of non-Newtonian fluid flow has become a hot area of research because traditional Newtonian fluids often fail to accurately model the behaviour of fluids in various industrial applications. Biological fluids, polymeric fluids, fluids containing additives, liquid crystals, and

Received July. 20, 2025

2020 Mathematics Subject Classification. 76A05.

*Key words and phrases.* micropolar nanofluid; stretching/shrinking surface; thermal radiations; soret effect; chemical reaction; stability analysis.

https://doi.org/10.28924/2291-8639-23-2025-290

© 2025 the author(s)

ISSN: 2291-8639

paint and colloidal solutions are all examples of non-Newtonian fluids that exhibit complex properties that cannot be captured by Newtonian fluid models. These fluids can be classified into different categories, including Casson fluids, Maxwell fluids, and micropolar fluids, each with unique characteristics.

Understanding the behaviour of these non-Newtonian fluids is crucial for accurately modelling and simulating various industrial processes, such as fluid flow, heat transfer, and mass transport. By recognizing the limitations of Newtonian fluids and exploring the properties of non-Newtonian fluids, researchers and engineers can develop more accurate and effective solutions for a wide range of applications. Eringen [1] provides a framework to understand the behaviour of fluids with particles exhibiting both microstructure and micro motion, allowing the prediction of complex fluid behavior in various engineering and biological applications. He also presents experimental evidence supporting the newly introduced micro-deformation rate tensors, an essential element in formulating constitutive equations for microfluidic systems.

Parametric analysis of micropolar fluid flow with thermal radiation over a porous stretching surface was studied by Bilal et al. [2]. The physical behavior of micropolar nanofluid flow over a porous plate with uniform motion was examined by Stepha et al. [3]. Simulation of micropolar liquid flow and energy transfer through permeable plates using numerical methods was explored by Pasha et al. [4]. Energy transfer and fluid flow of a micropolar liquid driven by a permeable extending surface was studied by Turkyilmazoglu [5].

Micropolar nanofluid flow over a permeable stretching sheet with suction was inspected by Fauzi et al. [6]. Micropolar liquid flow in a porous medium with suction towards a linearly stretching/shrinking sheet was explored by Rosali et al. [7]. Nanotechnology's vast potential has sparked widespread interest among researchers due to its potential to revolutionize industries and enhance medical outcomes.

The industry utilizes nanotechnology to develop advanced materials, such as clay nanocomposites for impermeable films, silver nanoparticles for antimicrobial storage, zinc oxide particles for UV shielding, and carbon nanotube-infused graphite for exceptionally lightweight tennis rackets. In the medical field, researchers are developing nanocapsules as a promising alternative to traditional injections, designed to traverse the stomach and enter the bloodstream directly. Additionally, nanoparticles with antibacterial properties are being coupled to create advanced wound dressings and bandages for cuts and stitches.

The field of nanotechnology includes a fascinating subclass known as nanofluids, holding significant potential for innovation and discovery. According to Choi [8], nanotechnology is extensively utilized in various fields, including transportation, biomedicine, electronics, and nuclear reactors, due to its exceptional heat transfer properties, which have revolutionized the respective industries.

Nanofluids are created by dispersing nano-scale particles (typically between 1-100 nanometers in size) in traditional fluids, resulting in enhanced fluid properties and behavior. Researchers have made significant contributions, investigating nanofluid flow dynamics over stretching and shrinking surfaces, with promising applications in engineering and technology, as seen in Buongiorno and Hu [9] two-phase nanofluid model and other studies [10-12].

The study of magnetohydrodynamics is essential for understanding the behaviour of electrically conducting fluids, known as MHD fluids, which interact with magnetic fields. MHD fluids have diverse applications in fusion energy, plasma cutting, electromagnetic pumping, magnetorheological fluids, biomedical applications, and various industries. MHD plays a vital role in fluid dynamics, metallurgical science, aerodynamics, and engineering disciplines, controlling convection processes like metal casting, nuclear reactor safety, and material manufacturing through magnetic field manipulation. The vast potential of MHD has captured the attention of researchers, leading to substantial progress and innovations in the field. Magnetohydrodynamic flow and energy transfer of micropolar nanofluid over a linearly extending/shrinking porous surface were studied by Kumar et al. [13].

Dual solutions for the mathematical model of MHD flow of micropolar nanoliquid past a vertical shrinking surface under the influence of buoyancy forces were probed by Lund et al. [14]. Numerical investigation of MHD nanofluid flow over a stretching/shrinking surface with heat radiation was examined by Mohanty et al. [15]. MHD flow and radiation effects on micropolar nanoliquid over a stretching/shrinking sheet were inspected by Patel et al. [16]. MHD flow and energy transfer of micropolar nanoliquid over an exponentially stretching/shrinking surface were considered by Dero et al. [17].

In the current era of sustainable development and technological progress, the significance of heat and mass transfer within boundary layer flows has become more essential, driving innovation and advancements in various industries. As the world tackles energy crises, environmental pollution, and food security challenges, the optimization of heat and mass transfer processes in boundary layers has become a critical factor in the design and operation of various industrial systems.

From enhancing heat transfer in solar collectors and bioreactors to improving mass transfer in chemical processing, water treatment plants, pharmaceutical manufacturing, food processing, aerospace engineering, and automotive systems, the efficient management of boundary layer flow is essential for achieving energy efficiency, reducing emissions, and promoting sustainable development.

By understanding and controlling heat and mass transfer in boundary layers, we can unlock new possibilities for innovation and progress in a wide range of industries, including energy generation, chemical production, environmental remediation, and advanced materials development. Numerous researchers have made significant contributions to this field, including the work on boundary layer control and the development of heat transfer. Fatima et al. [18] investigated the transport of energy and mass in a boundary layer flow induced by motile gyrotactic microorganisms swimming near a flat plate with variable wall temperature. Kebede et al. [19] researched the transport phenomena of energy and mass in unsteady boundary layer flow of Williamson nanofluids.

Sharma et al. [20] analyzed the impact of convective heat and mass conditions on the dynamics of MHD boundary layer flow with thermal radiation and Joule heating. Long et al. [21] conducted a study on Marangoni boundary layer flow and heat transfer with innovative constitutive relationships. Ferdows et al. [22] performed a comprehensive three-dimensional analysis of boundary layer flow and heat/mass transfer in stagnation point flow of hybrid nanofluid.

Arif et al. [23] presented a numerical study using a modified finite element method to analyze energy and mass transfer in MHD non-Newtonian boundary layer flow of nanoliquids with electrical conductivity. Ullah et al. [24] developed a soft computing model to simulate energy and mass transfer properties of nanoliquid in MHD boundary layer flow above an upright cone with convective boundary conditions. Khan et al. [25] investigated the effects of heat and mass transfer on the unsteady boundary layer flow of a chemically reacting Casson fluid.

Heat generation/absorption is an interesting phenomenon that has captivated the attention of scientists across various disciplines. As a crucial aspect of thermal management, heat generation/absorption plays a vital role in understanding and optimizing energy transfer, conversion, and storage. By exploring into the complexities of heat generation/ absorption, researchers can uncover novel insights into thermodynamic processes, material properties, and technological innovations.

From enhancing energy efficiency and reducing emissions to advancing nuclear reactor design and safety, the scientific exploration of heat generation/absorption offers a rich landscape of opportunities for groundbreaking discoveries and applications.

As a consequence, scientists and engineers are excited to investigate and uncover the complex aspects of heat generation and absorption, driving innovation and progress in this exciting field. Mondal et al. [26] conducted a study on heat generation/absorption in MHD double diffusive mixed convection of different nanofluids in a trapezoidal enclosure. Yasir et al. [27] studied the effects of heat generation/absorption on thermally radiative mixed convective movement of  $Zn - TiO_2/H_2O$  hybrid nanofluid.

Kumar et al. [28] analyzed the impact of heat generation/absorption on the mixed convection flow field in a vertical channel with a permeable matrix. Reddy et al. [29] studied the heat absorption/generation effects on MHD heat transfer fluid flow along a stretching cylinder with a porous medium. Goud [30] explored the effect of heat generation/absorption on MHD flow of a

micropolar fluid through a porous medium with a permeable surface and variable suction/injection. Soomro et al. [31] inspected the effects of heat generation/absorption and nonlinear radiation on the stagnation point flow of a nanoliquid above a moving surface.

This study addresses a knowledge gap in the existing literature by investigating the energy and mass transport phenomena of micropolar nanofluid flow, considering the combined effects of inclined magnetic field, chemical reaction, and Soret effect over a permeable stretching/shrinking surface.

The Buongiorno's model gives us a great deal of flexibility in analysing Brownian motion and thermophoretic effects on the flow of micropolar nanofluid. The study focuses on the triple solutions of the flow phenomenon and their stability, using the Stability Analysis method. The findings are presented in a detailed and organized manner, showcasing the effects of key parameters through graphs and tables.

#### 2. Mathematical Formulation

Consider the steady two-dimensional MHD flow of heat and mass transfer of micropolar nanofluid over a porous stretching/shrinking surface in the presence of heat generation/absorption and the Soret effect. The surface velocity is assumed to be  $u_{w(x)} = \lambda x$ , where  $\lambda > 0$  represents the stretching case and  $\lambda < 0$  the shrinking case. The x-axis aligned along the surface and the y-axis directed normal to it. The flow is confined to the region y > 0. The surface is porous, with a mass flux velocity  $v_0$ , where  $v_0 < 0$  represents suction and  $v_0 < 0$  represents injection. A magnetic field  $B_0$  is applied along the y-axis. The wall maintains a constant temperature  $T_w$  and concentration  $C_w$ , while the ambient temperature  $T_\infty$  and concentration  $C_\infty$  of the nanoliquid vary as  $y \to \infty$ , as shown in Figure 1.

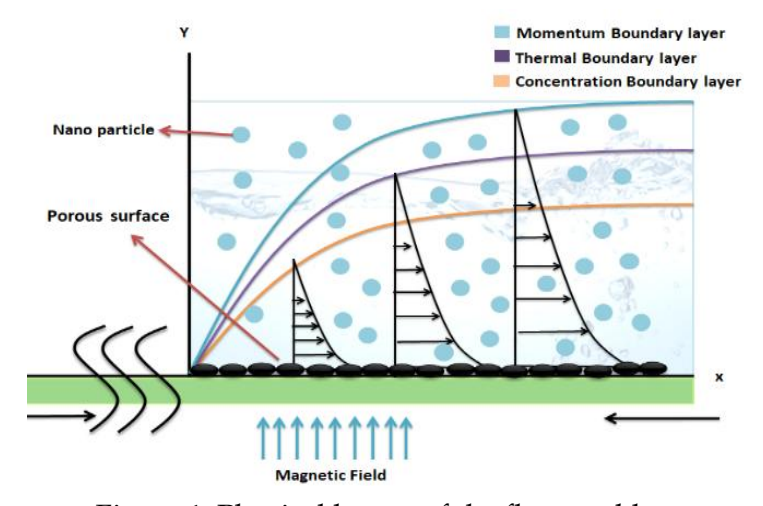


Figure 1. Physical layout of the flow problem

By applying the appropriate boundary layer approximations and based on the conditions specified above, the governing equations for the boundary layer can be expressed as seen in Kumar et al. [32], Sharma et al. [33], Abbas et al. [34], and Pasha et al. [35]

$$\frac{\partial u}{\partial x} + \frac{\partial v}{\partial y} = 0 \tag{1}$$

$$u\frac{\partial u}{\partial x} + v\frac{\partial u}{\partial y} = \left(v + \frac{k}{\rho}\right)\frac{\partial^2 u}{\partial y^2} + \frac{k}{\rho}\frac{\partial N}{\partial y} - \frac{\sigma B_0^2}{\rho}u\cos\gamma, \qquad (2)$$

$$u\frac{\partial N}{\partial x} + v\frac{\partial N}{\partial y} = \frac{1}{\rho j} \left[ \gamma \frac{\partial^2 N}{\partial y^2} - k \left( 2N + \frac{\partial u}{\partial y} \right) \right] \tag{3}$$

$$u\frac{\partial T}{\partial x} + v\frac{\partial T}{\partial y} = \left(\alpha + \frac{16\sigma^* T_{\infty}^3}{3k^* \rho C_p}\right)\frac{\partial^2 T}{\partial y^2} + \tau \left[D_B \frac{\partial C}{\partial y} \frac{\partial T}{\partial y} + \frac{D_T}{T_{\infty}} \left(\frac{\partial T}{\partial y}\right)^2\right] + \frac{Q_o}{\rho C_p} (T - T_{\infty}) \tag{4}$$

$$u\frac{\partial C}{\partial x} + v\frac{\partial C}{\partial y} = D_B \frac{\partial^2 C}{\partial y^2} + \frac{D_T K_T}{T_{\infty}} \frac{\partial^2 T}{\partial y^2} - R^*(C - C_{\infty}). \tag{5}$$

With the boundary conditions

$$v = v_o; u = \lambda u_w(x); N = -m \frac{\partial u}{\partial y}; T = T_W; C = C_W \text{ (at } y=0)$$

$$u \to 0; N \to 0; T \to T_\infty; C \to C_\infty \text{ as } y \to \infty$$
(6)

The following similarity transformation can be applied to rewrite the equations for momentum, angular momentum, and energy into corresponding ODE.

$$u = axf'(\eta), \ v = -\sqrt{ax}f(\eta), \ \eta = y\sqrt{\frac{a}{v}}, \ N = \sqrt{\frac{a}{v}}axg(\eta)$$
 (7)

The similarity variable  $\eta = \eta(x, y)$ , transforms the original partial differential equation (PDE) into a nonlinear ODE, which

$$(1+K)f''' + ff'' - f'^2 + Kg' - Mf' = 0, (8)$$

$$\left(1 + \frac{K}{2}\right)g'' + g'f - gf' - 2Kg - Kf'' = 0 \tag{9}$$

$$\frac{1}{Pr} \left( 1 + \frac{4}{3} Rd \right) \theta'' + f \theta' + N_b \phi' \theta' + N_t \theta'^2 + Q\theta = 0$$
 (10)

$$\emptyset'' + Sc(f\emptyset' + Sr\theta'' - R\emptyset) = 0. \tag{11}$$

After applying the similarity transformation, the original boundary conditions are characterized by the following transformed boundary conditions at  $\eta \to \infty$ :

$$f(0) = f_w; \ f'(0) = \lambda; \ g(0) = -mf''(0); \ \theta(0) = 1;$$
  
$$\phi(0) = 1 \ f'(\eta) \to 0; \ g(\eta) \to 0; \ \theta(\eta) \to 0; \ \phi(\eta) \to 0$$
 (12)

Whereas, primes represent the differentiation with respect to  $\eta$ ,  $K=\frac{k}{\mu}$ , is the parameter for micropolar materials  $Pr=\frac{\vartheta}{a}$ , is the Prandtl number,  $M=\frac{\sigma B_0^2}{\rho a}$ , is the Magnetic parameter,  $R_d=\frac{4\sigma T_\infty^3}{K^*k}$ , is a thermal radiation parameter,  $N_b=\frac{\tau_W D_B(C_W-C_\infty)}{v}$ , stands for Brownian motion parameter,  $N_t=\frac{\tau_W D_T(T_W-T_\infty)}{vT_\infty}$ , is the thermophoresis diffusion parameter,  $Q=\frac{Q_0}{\rho C_p a}$ , is the heat generation/absorption coefficient,  $Sr=\frac{D_T K_T(T_W-T_\infty)}{vT_\infty(C_W-C_\infty)}$ , indicates the Soret factor and  $Sc=\frac{\vartheta}{D_B}$ , is stands for Schmidt number. Additionally,  $f_W=\frac{-v_0}{\sqrt{a\vartheta}}$ , is the suction factor  $(f_W>0)$ .

The quantities of physical interest in this study are the skin friction factor  $C_f$ , local Nusselt number  $N_u$  and Sherwood number  $S_h$  which are defined as:

$$C_f = \frac{\left[ (\mu + k) \frac{\partial u}{\partial y} + kN \right]_{y=0}}{\rho u_W^2}, N_u = \frac{-x \left[ \left( \frac{16\sigma^* T_\infty^3}{3K^*} + k \right) \frac{\partial T}{\partial y} \right]_{y=0}}{(T_W - T_\infty)}, S_h = \frac{-x \left( \frac{\partial C}{\partial y} \right)_{y=0}}{(C_W - C_\infty)}$$

$$(13)$$

By inserting (12) into (13), we get:

$$C_{f}(Re_{x})^{\frac{1}{2}} = (1 + (1 - m)K)f''(0), N_{u}(Re_{x})^{-\frac{1}{2}} = -\left(1 + \frac{4}{3}Rd\right)\theta'(0), S_{h}(Re_{x})^{-\frac{1}{2}} = -\emptyset'(0),$$
(14)

Where,  $Re_x = \frac{ax^2}{\vartheta}$  is a local Reynolds number.

## 3. Stability Analysis

A stability analysis is essential to determine the stable and physically realistic solution, as it helps to identify the solution for both mathematically valid and physically meaningful. Using the approach presented in Norzawary et al. [36] and Rafique et al. [37]. Equations (2) to (5) are converted into unsteady form by introducing the time-dependent variable  $\tau$ . The continuity (1) satisfied and additional PDEs are introduced:

$$\frac{\partial u}{\partial t} + u \frac{\partial u}{\partial x} + v \frac{\partial u}{\partial y} = \left(v + \frac{\kappa}{\rho}\right) \frac{\partial^2 u}{\partial y^2} + \frac{\kappa}{\rho} \frac{\partial N}{\partial y} - \frac{\sigma B_0^2}{\rho} u \cos \gamma, \tag{15}$$

$$\frac{\partial N}{\partial t} + u \frac{\partial N}{\partial x} + v \frac{\partial N}{\partial y} = \frac{1}{\rho_i} \left[ \gamma \frac{\partial^2 N}{\partial y^2} - K \left( 2N + \frac{\partial u}{\partial y} \right) \right],\tag{16}$$

$$\frac{\partial T}{\partial t} + u \frac{\partial T}{\partial x} + v \frac{\partial T}{\partial y} = \left(\alpha + \frac{16\sigma^* T_{\infty}^3}{3k^* \rho c_p}\right) \frac{\partial^2 T}{\partial y^2} + \tau \left[D_B \frac{\partial C}{\partial y} \frac{\partial T}{\partial y} + \frac{D_T}{T_{\infty}} \left(\frac{\partial T}{\partial y}\right)^2\right] + \frac{Q_0}{\rho c_p} (T - T_{\infty}), \tag{17}$$

$$\frac{\partial C}{\partial t} + u \frac{\partial C}{\partial x} + v \frac{\partial C}{\partial y} = D_B \frac{\partial^2 C}{\partial y^2} + \frac{D_T}{T_{\infty}} K_T \frac{\partial^2 T}{\partial y^2} - R^* (C - C_{\infty}). \tag{18}$$

A new similarity transformation is now obtained as follows

$$\eta = y \sqrt{\frac{a}{v}}; \ \tau = at; \ u = \frac{ax\partial f(\eta, \ \tau)}{\partial \eta}; \ v = -\sqrt{av}f(\eta, \tau); \ N = \sqrt{\frac{a}{v}}axg(\eta, \tau); 
\theta(\eta, \tau) = \frac{T - T_{\infty}}{T_{w} - T_{\infty}}; \ \phi(\eta, \tau) = \frac{C - C_{\infty}}{C_{w} - C_{\infty}}$$
(19)

The following system is obtained by applying (19) into (15) to (18)

$$(1+K)\frac{\partial^3 f}{\partial \eta^3} + f\frac{\partial^2 f}{\partial \eta^2} - \left(\frac{\partial f}{\partial \eta}\right)^2 + K\frac{\partial g}{\partial \eta} - M\frac{\partial f}{\partial \eta}\cos\gamma - \frac{\partial^2 f}{\partial \tau \partial \eta} = 0,$$
(20)

$$\left(1 + \frac{K}{2}\right)\frac{\partial^2 g}{\partial n^2} + f\frac{\partial g}{\partial n} - g\frac{\partial f}{\partial n} - 2Kg - K\frac{\partial^2 f}{\partial n^2} - \frac{\partial g}{\partial \tau} = 0,\tag{21}$$

$$\frac{1}{Pr} \left( 1 + \frac{4}{3} R d \right) \frac{\partial^2 \eta}{\partial \eta^2} + f \frac{\partial \theta}{\partial \eta} + N_b \frac{\partial \theta}{\partial \eta} \frac{\partial \phi}{\partial \eta} + N_t \left( \frac{\partial \theta}{\partial \eta} \right)^2 + Q \theta - \frac{\partial \theta}{\partial \tau} = 0$$
 (22)

$$\frac{\partial^2 \phi}{\partial \eta^2} + Sc \left( f \frac{\partial \phi}{\partial \eta} + Sr \frac{\partial^2 \theta}{\partial \eta^2} - R \frac{\partial \phi}{\partial \eta} \right) - \frac{\partial \phi}{\partial \tau} = 0. \tag{23}$$

Subjected to the boundary conditions

$$f(0,\tau) = S$$
,  $\frac{\partial f(0,\tau)}{\partial \eta} = \lambda$ ,  $g(0,\tau) = -m \frac{\partial^2 f(0,\tau)}{\partial \eta^2}$ ,

$$\theta(0,\tau) = 1, \ \phi(0,\tau) = 1 \ \text{at} \quad \eta \to 0, \frac{\partial f(0,\tau)}{\partial \eta} \to 0,$$
  
$$g(\eta,\tau) \to 0, \ \theta(\eta,\tau) \to 0, \ \phi(\eta,\tau) \to 0 \ \text{as} \ \eta \ \infty.$$
 (24)

The fundamental solutions have now been modified to

$$f(\eta) = f_0(\eta), g(\eta) = g_0(\eta), \theta(\eta) = \theta_0(\eta)$$
 and  $\phi(\eta) = \phi_0(\eta),$ 

through disorders as

$$f(\eta, \tau) = f_0(\eta) + e^{-\varepsilon \tau} F(\eta),$$

$$g(\eta, \tau) = g_0(\eta) + e^{-\varepsilon \tau} G(\eta),$$

$$\theta(\eta, \tau) = \theta_0(\eta) + e^{-\varepsilon \tau} H(\eta),$$

$$\phi(\eta, \tau) = \phi_0(\eta) + e^{-\varepsilon \tau} S(\eta).$$
(25)

Assuming  $F(\eta)$ ,  $G(\eta)$ ,  $H(\eta)$  and  $S(\eta)$  are small compared to  $f_0(\eta)$ ,  $g_0(\eta)$ ,  $\theta_0(\eta)$  and  $\phi_0(\eta)$ , and  $\varepsilon$  is the smallest eigenvalue, we obtain the linearized eigenvalue as a result.

$$(1+K)F_0''' + f_0F_0'' + F_0f_0'' - 2f_0'G_0' + KG_0' - MF_0'\cos\gamma + \varepsilon F_0' = 0, \tag{26}$$

$$\left(1 + \frac{K}{2}\right)G_0^{\prime\prime} + f_0G_0^{\prime} + F_0g_0^{\prime} - g_0F_0^{\prime} - G_0f_0^{\prime} - KG_0 - KF_0^{\prime\prime} + \varepsilon G_0 = 0, \tag{27}$$

$$\frac{1}{Pr} \left( 1 + \frac{4}{3} Rd \right) H_0^{\prime\prime} + f_0 H_0^{\prime} + F_0 \theta_0^{\prime} + N_b \phi_0^{\prime} H_0^{\prime} + N_b S_0^{\prime} \theta_0^{\prime} + 2N_t \theta_0^{\prime} H_0^{\prime} + Q H_0^{\prime} + \varepsilon H_o = 0,$$
 (28)

$$S_0'' + Sc(f_0S_0' + F_0\emptyset_0') + ScS_rH_0'' - ScR\emptyset_0' + \varepsilon S_0 = 0.$$
(29)

Subject to the following boundary conditions as  $\eta \to \infty$ 

$$F_0(0) = 0, F_0'(0) = 0, G_0(0) = -mF_0''(0), H_0(0) = 0$$

$$S_0(0) = 0, F_0'(\eta) \to 0, G_0(\eta) \to 0, H_0(\eta) \to 0, S_0(\eta) \to 0$$
(30)

Utilizing MATLAB using the BVP4c solver function, we solve the linearized solutions (26) to (29) with the boundary conditions (30) to compute the values of the least eigenvalue  $\varepsilon$ . To address the current problem, we relax the condition that  $G_0(\eta) \to 0$  as  $\eta \to \infty$ . Moreover, we impose the extra boundary condition to solve the system (26) to (29).

#### 4. Results and Discussion

The nonlinear system of ODEs (8) to (11), subject to the boundary conditions (12), has been numerically solved using the bvp4c function in MATLAB, which is an effective technique for data analysis. The numerical study has been performed to consider the fluid flow model, focusing on the influence of various significant physical parameters such as magnetic parameter M, Micropolar material factor K, Radiation impact parameter Rd, Brownian motion parameter  $N_b$ , thermophoresis parameter  $N_t$ , Soret effect parameter  $S_r$ , Heat generation/absorption Q respectively.

We verify the accuracy of our stability analysis by comparing our results with prior research (comparison  $(C_f(Re_x)^{\frac{1}{2}})$  and variation of K as mentioned in Table 1) and previously published literature by Dero et al. [38] achieving excellent agreement and confirming the validity of our numerical outcomes. Table 2 lists the values of S and K for various  $\varepsilon$  values. This verification

4

-2.005420

enhances our confidence in the conclusions. Within specific parameter ranges, triple solutions become attainable. The first solution, with  $\varepsilon > 0$ , is deemed stable and physically important. We base our results on this solution, although the second and third solutions (with  $\varepsilon < 0$ ) holds mathematical significance.

	m=0		m=0.5		
K	Dero et al. [38]	Present	Dero et al. [38]	Present	
0	-1.00000	-1.00012	-1.00000	-1.00000	
1	1.367996	1.367985	-1.224819	-1.224819	
2	-1.621570	-1.621570	-1.414479	-1.414479	

-2.005420

Table 1. The effect of k on  $(C_f(Re_x)^{\frac{1}{2}})$  with  $M=Q=Sr=R=\gamma=0$ 

Table 2. Smallest eigenvalues corresponding to different values of k and s

-1.733292

-1.733292

ε						
K	S	1 <sup>st</sup> Solution	2 <sup>nd</sup> Solution	3 <sup>rd</sup> Solution		
0	3	0.65232	-1.04592	-0.36212		
0	2.5	0.39380	-0.77841	-0.45736		
0	2	0.03269	-0.13870	-0.03257		
1	3	0.49827	-0.85106	-0.37857		
1	2.5	0.14281	-0.49401	-0.13000		
2	3	0.26092	-0.52380	-0.23062		

The velocity profile in Figure 2 shows a decrease with rising *M*, which reduces the boundary layer thickness associated with the first solution. The Lorentz force, generated by the interaction between the conducting liquid and the magnetic field, acts on the fluid particles, restricting their momentum and leading to the observed results. A similar influence is expected on the second and third solutions, as the enhanced Lorentz force will continue to restrict the fluid particles' momentum, yielding comparable effects on the velocity profiles and boundary layer thickness.

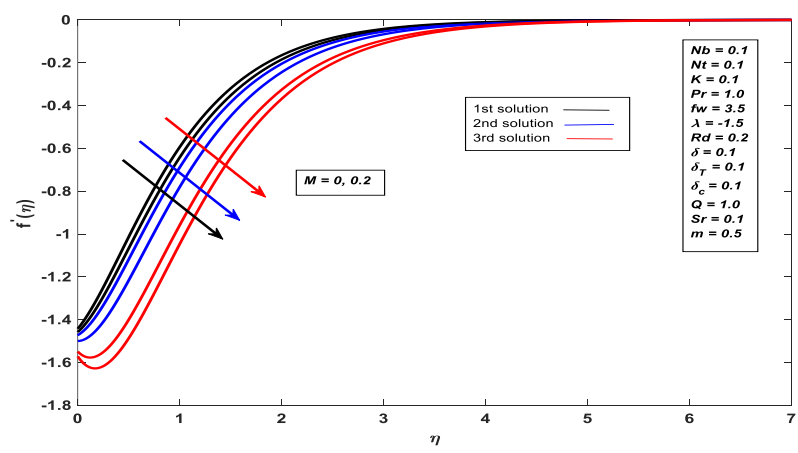


Figure 2.The effects of *M* on the velocity distribution.

Figure 3 illustrates the influence of *K* on the velocity profile, showing the changes in velocity distribution for different *K* values. Our analysis reveals an inverse relationship between *K* and velocity for the first solution, where higher *K* values correspond to lower velocities and reduced boundary layer momentum thickness. In contrast, the second and third solutions exhibit a direct relationship between *K* and velocity, where increasing *K* values lead to higher velocities. This phenomenon is attributed to the increase in fluid viscosity with rising material rate, resulting in higher flow resistance due to the fluid's increased thickness and resistance to motion.

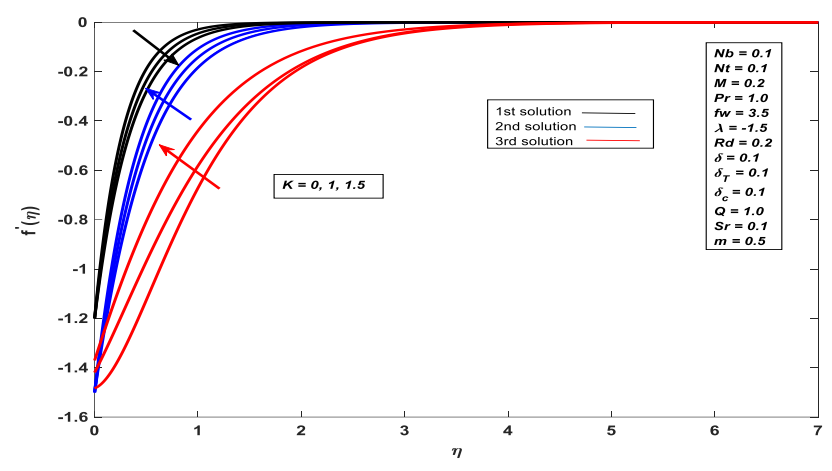


Figure 3. The effects of K on the velocity distribution

Figure 4 illustrates the impact of K on the microrotation profiles, demonstrating how variations in K shape the microrotation distribution. For the first and second solutions, increasing K leads to a reduction in both the microrotation boundary layer thickness and the micropolar profiles, indicating a suppressing effect of K on microrotation. In contrast, the third solution exhibits a fluctuating behavior, where the nanofluid's velocity initially decreases but ultimately increases as K is increased, suggesting a complex interplay between K and microrotation in this case.

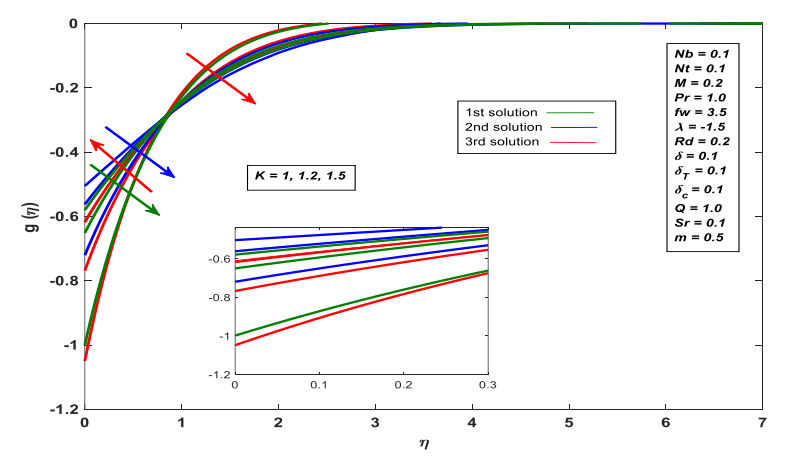


Figure 4. The effects of *K* on the microrotation distribution

Figure 5 illustrates the effect of thermal radiation on the temperature distribution, with the thermal radiation factor *Rd* characterizing the interplay between conduction and radiation in energy transfer. Increasing the thermal radiation rate leads to a decrease in both the thermal boundary layer thickness and the heat transfer rate, consistently across all solutions. This indicates that enhanced thermal radiation weakens the thermal boundary layer, thereby reducing heat transfer.

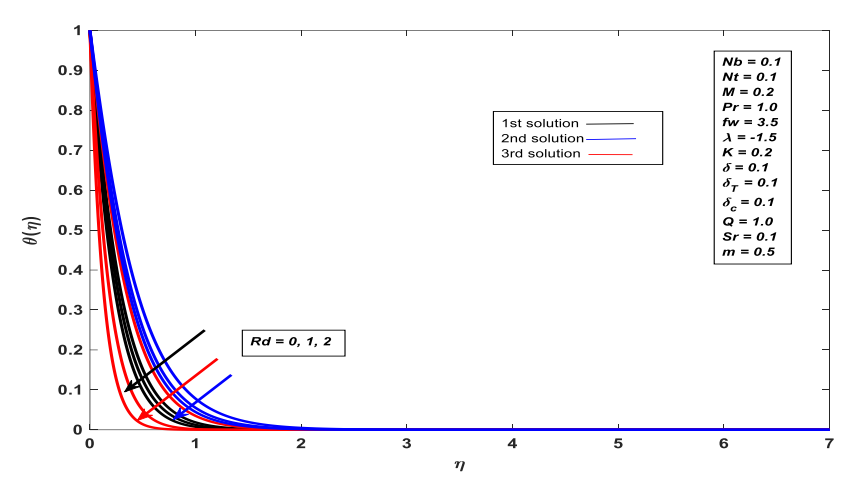


Figure 5. The effects of Rd on temperature distribution

Figure 6 shows that the temperature of the micropolar nanofluid increases as the Brownian motion parameter  $N_b$  increases. "This is caused by the collective influence of growing nanoparticle percentage and the impact of the Brownian motion parameter." Additionally, the influence of increasing  $N_t$  on the thermal conductivity of nanoparticles in the base fluid is examined, resulting in increased temperature distributions and thermal boundary layer thickness for the 1st and 3rd solutions, but a decrease for 2nd solution as in Figure 7.

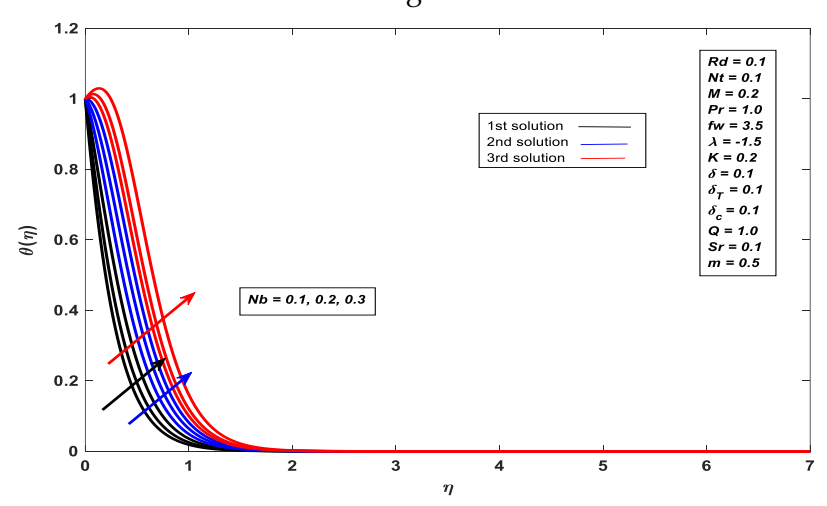


Figure 6. The effects of Nb on temperature distribution

Figure 8 illustrates the influence of the Soret effect parameter on the concentration distribution. In all three solutions, a consistent trend emerges: an increase in the Soret effect leads to a more pronounced concentration distribution near the boundary, resulting in a thicker boundary layer. This enhanced concentration distribution is evident in the increased thickness of the boundary layer

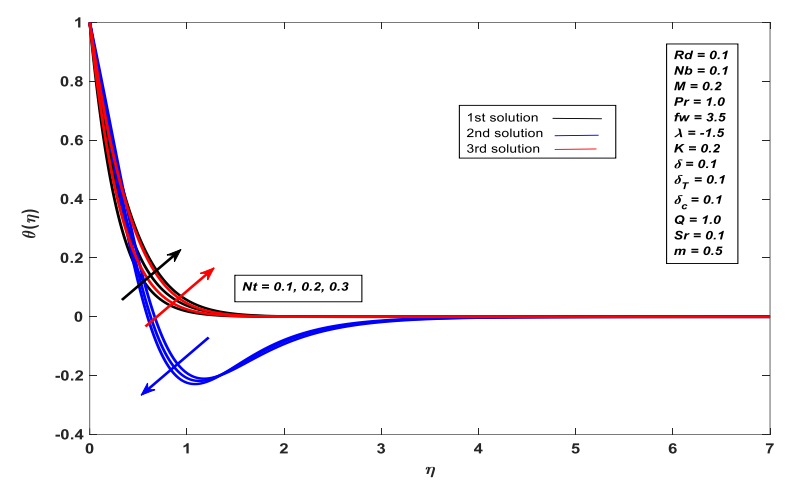


Figure 7. The effects of Nt on temperature distribution

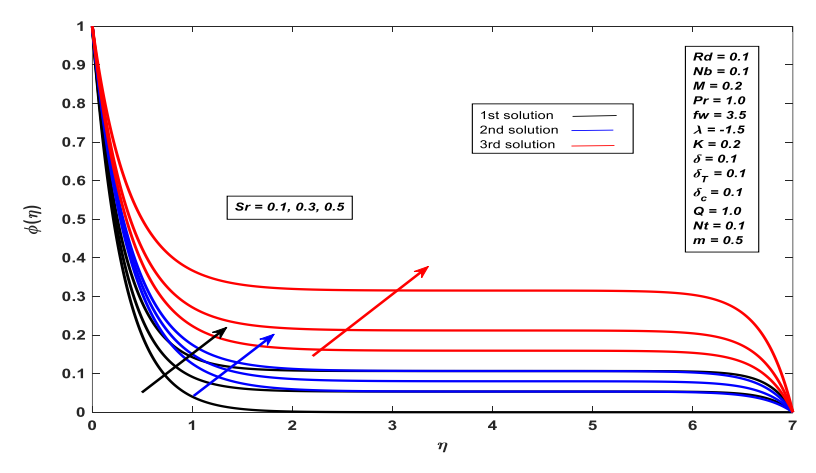


Figure 8. The effects of Sr on concentration distribution.

### 5. Conclusions

This study examines the effects of heat generation/absorption and the Soret effect on the steady, two-dimensional, laminar flow of heat and mass transfer of micropolar nanofluid in the boundary layer flow over a linearly stretching/shrinking surface. Using similarity transformation, the governing equations are reduced to ordinary differential equations, revealing the physical properties of the micropolar nanofluid flow, including radiation, micropolar material and thermophoresis parameters, and Brownian motion. The key findings of this research are:

- 1. Through stability analysis, it is determined that the first solution is stable and feasible from a physical perspective, whereas the second and third solutions are unstable and therefore not feasible in practice.
- 2. The analysis shows that the microrotation profiles and boundary layer thicknesses in the first two solutions decrease with increasing *K*, however there is a variation in the third solution.
- 3. The temperature profile decreases with increased thermal radiation factor, whereas increase with increasing Brownian motion factor, and thermophoresis has a mixed impact on boundary layer thickness, improving in the 1st and 3rd solutions but decreasing in the 2rd solution."
- 4. The concentration of nanoparticles increases with increasing Soret effect parameter (Sr), as the Soret effect enhances the migration of nanoparticles to the boundary layer.

**Acknowledgments:** The authors extend their appreciation to the Arab Open University for funding this work.

**Conflicts of Interest:** The authors declare that there are no conflicts of interest regarding the publication of this paper.

#### References

- [1] A.C. Eringen, Theory of Micropolar Elasticity, in: Microcontinuum Field Theories, Springer New York, New York, NY, 1999: pp. 101-248. https://doi.org/10.1007/978-1-4612-0555-5\_5.
- [2] M. Bilal, A. Saeed, T. Gul, W. Kumam, S. Mukhtar, et al., Parametric Simulation of Micropolar Fluid with Thermal Radiation Across a Porous Stretching Surface, Sci. Rep. 12 (2022), 2542. https://doi.org/10.1038/s41598-022-06458-3.
- [3] N.G. Stepha, D.K. Jacob, Analysis on Physical Properties of Micropolar Nanofluid Past a Constantly Moving Porous Plate, IOP Conf. Ser.: Mater. Sci. Eng. 1206 (2021), 012004. https://doi.org/10.1088/1757-899x/1206/1/012004.
- [4] P. Pasha, S. Mirzaei, M. Zarinfar, Application of Numerical Methods in Micropolar Fluid Flow and Heat Transfer in Permeable Plates, Alex. Eng. J. 61 (2022), 2663-2672. https://doi.org/10.1016/j.aej.2021.08.040.
- [5] M. Turkyilmazoglu, Flow of a Micropolar Fluid Due to a Porous Stretching Sheet and Heat Transfer, Int. J. Nonlinear Mech. 83 (2016), 59-64. https://doi.org/10.1016/j.ijnonlinmec.2016.04.004.
- [6] E.L.A. Fauzi, S. Ahmad, I. Pop, Flow Over a Permeable Stretching Sheet in Micropolar Nanofluids with Suction, AIP Conf. Proc. 1605 (2014), 428-433. https://doi.org/10.1063/1.4887627.
- [7] H. Rosali, A. Ishak, I. Pop, Micropolar Fluid Flow Towards a Stretching/shrinking Sheet in a Porous Medium with Suction, Int. Commun. Heat Mass Transf. 39 (2012), 826-829. https://doi.org/10.1016/j.icheatmasstransfer.2012.04.008.
- [8] S.U.S. Choi, Nanofluids: A New Field of Scientific Research and Innovative Applications, Heat Transf. Eng. 29 (2008), 429-431. https://doi.org/10.1080/01457630701850778.

- [9] J. Buongiorno, L. Hu, Innovative Technologies: Two-Phase Heat Transfer in Water-Based Nanofluids for Nuclear Applications: Final Report, Nuclear Engineering Education Research (NEER) Program, Office of Scientific and Technical Information (OSTI), 2009. https://doi.org/10.2172/958216.
- [10] K.R. Jahnavi, G.S. Hegde, A Review on Nano Fluid Production, Mathematical Modelling and Applications, J. Nanofluids 13 (2024), 269-305. https://doi.org/10.1166/jon.2024.2138.
- [11] A. Svobodova-Sedlackova, A. Calderón, C. Barreneche, R. Salgado-Pizarro, P. Gamallo, et al., A Bibliometric Analysis of Research and Development of Nanofluids, J. Nanofluids 12 (2023), 157-172. https://doi.org/10.1166/jon.2023.1924.
- [12] R. Barai, D. Kumar, A. Wankhade, Heat Transfer Performance of Nanofluids in Heat Exchanger: A Review, J. Therm. Eng. 9 (2023), 86-106. https://doi.org/10.18186/thermal.1243398.
- [13]S. Kumar, A.A. Shaikh, H.B. Lanjwani, S.F. Shah, MHD Flow and Heat Transfer of Micropolar Nanofluid on a Linearly Stretching/shrinking Porous Surface, VFAST Trans. Math. 11 (2023), 141-154. https://doi.org/10.21015/vtm.v11i1.1456.
- [14] L.A. Lund, Z. Omar, I. Khan, Mathematical Analysis of Magnetohydrodynamic (MHD) Flow of Micropolar Nanofluid Under Buoyancy Effects Past a Vertical Shrinking Surface: Dual Solutions, Heliyon 5 (2019), e02432. https://doi.org/10.1016/j.heliyon.2019.e02432.
- [15] B. Mohanty, S. Jena, P.K. Pattnaik, MHD Nanofluid Flow Over Stretching/Shrinking Surface in Presence of Heat Radiation Using Numerical Method, Int. J. Emerg. Technol. 10 (2019), 119-125.
- [16] H.R. Patel, A.S. Mittal, R.R. Darji, MHD Flow of Micropolar Nanofluid Over a Stretching/Shrinking Sheet Considering Radiation, Int. Commun. Heat Mass Transf. 108 (2019), 104322. https://doi.org/10.1016/j.icheatmasstransfer.2019.104322.
- [17] S. Dero, A.M. Rohni, A. Saaban, MHD Micropolar Nanofluid Flow over an Exponentially Stretching/Shrinking Surface: Triple Solutions, J. Adv. Res. Fluid Mech. Therm. Sci. 56 (2019), 165-174.
- [18] N. Fatima, W. Belhadj, K.S. Nisar, Usman, M.K. Alaoui, et al., Heat and Mass Transmission in a Boundary Layer Flow Due to Swimming of Motile Gyrotactic Microorganisms with Variable Wall Temperature Over a Flat Plate, Case Stud. Therm. Eng. 45 (2023), 102953. https://doi.org/10.1016/j.csite.2023.102953.
- [19] T. Kebede, E. Haile, G. Awgichew, T. Walelign, Heat and Mass Transfer in Unsteady Boundary Layer Flow of Williamson Nanofluids, J. Appl. Math. 2020 (2020), 1890972. https://doi.org/10.1155/2020/1890972.
- [20] R. Sharma, S. Tinker, B. Gireesha, B. Nagaraja, Effect of Convective Heat and Mass Conditions in Magnetohydrodynamic Boundary Layer Flow with Joule Heating and Thermal Radiation, Int. J. Appl. Mech. Eng. 25 (2020), 103-116. https://doi.org/10.2478/ijame-2020-0037.
- [21] Z. Long, L. Liu, S. Yang, L. Feng, L. Zheng, Analysis of Marangoni Boundary Layer Flow and Heat Transfer with Novel Constitution Relationships, Int. Commun. Heat Mass Transf. 127 (2021), 105523. https://doi.org/10.1016/j.icheatmasstransfer.2021.105523.
- [22] M. Ferdows, M. Shamshuddin, A.M. Rashad, M.G. Murtaza, S.O. Salawu, Three-Dimensional Boundary Layer Flow and Heat/mass Transfer Through Stagnation Point Flow of Hybrid Nanofluid, J. Eng. Appl. Sci. 71 (2024), 57. https://doi.org/10.1186/s44147-024-00388-9.

- [23] M.S. Arif, W. Shatanawi, Y. Nawaz, Modified Finite Element Study for Heat and Mass Transfer of Electrical MHD Non-Newtonian Boundary Layer Nanofluid Flow, Mathematics 11 (2023), 1064. https://doi.org/10.3390/math11041064.
- [24] H. Ullah, M. Shoaib, R.A. Khan, K.S. Nisar, M.A.Z. Raja, et al., Soft Computing Paradigm for Heat and Mass Transfer Characteristics of Nanofluid in Magnetohydrodynamic (MHD) Boundary Layer Over a Vertical Cone Under the Convective Boundary Condition, Int. J. Model. Simul. 45 (2023), 193-217. https://doi.org/10.1080/02286203.2023.2191586.
- [25] K.A. Khan, A.R. Butt, N. Raza, Effects of Heat and Mass Transfer on Unsteady Boundary Layer Flow of a Chemical Reacting Casson Fluid, Results Phys. 8 (2018), 610-620. https://doi.org/10.1016/j.rinp.2017.12.080.
- [26] P. Mondal, T.R. Mahapatra, R. Parveen, B.C. Saha, Heat Generation/Absorption in MHD Double Diffusive Mixed Convection of Different Nanofluids in a Trapezoidal Enclosure, J. Nanofluids 13 (2024), 339-349. https://doi.org/10.1166/jon.2024.2116.
- [27] M. Yasir, M. Khan, A. Alqahtani, M. Malik, Heat Generation/absorption Effects in Thermally Radiative Mixed Convective Flow of Zn-TiO2/H2O Hybrid Nanofluid, Case Stud. Therm. Eng. 45 (2023), 103000. https://doi.org/10.1016/j.csite.2023.103000.
- [28] K. Thanesh Kumar, S. Kalyan, M. Kandagal, J.V. Tawade, U. Khan, et al., Influence of Heat Generation/Absorption on Mixed Convection Flow Field with Porous Matrix in a Vertical Channel, Case Stud. Therm. Eng. 47 (2023), 103049. https://doi.org/10.1016/j.csite.2023.103049.
- [29] Y. Dharmendar Reddy, B. Shankar Goud, K.S. Nisar, B. Alshahrani, M. Mahmoud, et al., Heat Absorption/generation Effect on MHD Heat Transfer Fluid Flow Along a Stretching Cylinder with a Porous Medium, Alex. Eng. J. 64 (2023), 659-666. https://doi.org/10.1016/j.aej.2022.08.049.
- [30] B.S. Goud, Heat Generation/absorption Influence on Steady Stretched Permeable Surface on MHD Flow of a Micropolar Fluid Through a Porous Medium in the Presence of Variable Suction/injection, Int. J. Thermofluids 7-8 (2020), 100044. https://doi.org/10.1016/j.ijft.2020.100044.
- [31] F.A. Soomro, R.U. Haq, Q.M. Al-Mdallal, Q. Zhang, Heat Generation/Absorption and Nonlinear Radiation Effects on Stagnation Point Flow of Nanofluid Along a Moving Surface, Results Phys. 8 (2018), 404-414. https://doi.org/10.1016/j.rinp.2017.12.037.
- [32] S. Kumar, A.A. Shaikh, H.B. Lanjwani, S.F. Shah, MHD Flow and Heat Transfer of Micropolar Nanofluid on a Linearly Stretching/shrinking Porous Surface, VFAST Trans. Math. 11 (2023), 141-154. https://doi.org/10.21015/vtm.v11i1.1456.
- [33] S. Sharma, A. Dadheech, A. Parmar, J. Arora, Q. Al-Mdallal, et al., MHD Micro Polar Fluid Flow Over a Stretching Surface with Melting and Slip Effect, Sci. Rep. 13 (2023), 10715. https://doi.org/10.1038/s41598-023-36988-3.
- [34] A.A. Khan, M.N. Khan, N.A. Ahammad, et al., Flow Investigation of Second Grade Micropolar Nanofluid with Porous Medium Over an Exponentially Stretching Sheet, J. Appl. Biomater. Funct. Mater. 20 (2022), 22808000221089782. https://doi.org/10.1177/22808000221089782.
- [35] P. Pasha, S. Mirzaei, M. Zarinfar, Application of Numerical Methods in Micropolar Fluid Flow and Heat Transfer in Permeable Plates, Alex. Eng. J. 61 (2022), 2663-2672. https://doi.org/10.1016/j.aej.2021.08.040.

- [36] N.H. Adilla Norzawary, S.K. Soid, A. Ishak, M.K. Anuar Mohamed, U. Khan, et al., Stability Analysis for Heat Transfer Flow in Micropolar Hybrid Nanofluids, Nanoscale Adv. 5 (2023), 5627-5640. https://doi.org/10.1039/d3na00675a.
- [37] K. Rafique, G. Elkahlout, A.M. Saeed, Heat and Mass Transfer Analysis of Magnetized Micropolar Nanofluid Flow with Soret and Dufour Effects: Triple Solutions, Int. J. Anal. Appl. 23 (2025), 152. https://doi.org/10.28924/2291-8639-23-2025-152.
- [38] S. Dero, A.M. Rohni, A. Saaban, I. Khan, Dual Solutions and Stability Analysis of Micropolar Nanofluid Flow with Slip Effect on Stretching/Shrinking Surfaces, Energies 12 (2019), 4529. https://doi.org/10.3390/en12234529.